Scanning Microscopy

Volume 2 | Number 1 Article 16

9-12-1987

Electron Beam Testing of Passivated Devices via Capacitive Coupling Voltage Contrast

W. Reiners
Universität Duisburg

K. D. Herrman
Universität Duisburg

E. Kubalek
Universität Duisburg

Scanning Microscopy, Vol. 2, No. 1, 1988 (Pages 161-175)
Scanning Microscopy International, Chicago (AMF O'Hare), IL 60666 USA

0891-7035/88$3.00+.00

ELECTRON BEAM TESTING OF PASSIVATED DEVICES VIA CAPACITIVE COUPLING VOLTAGE CONTRAST

W. Reiners, K.D. Herrmann, E. Kubalek *

Universität Duisburg, Fachgebiet Werkstoffe der Elektrotechnik
Leiter: Prof. Dr.-Ing. E. Kubalek
Kommandantenstraße 60,
D-4100 Duisburg 1, F.R.G.

(Received for publication March 06, 1987, and in revised form September 12, 1987)

Abstract

By fundamental experiments and theoretical treatments a detailed understanding of the capacitive coupling voltage contrast (CCVC) has been gained, demontrating that this technique is, in principle, applicable to a non-destructive testing of passivated integrated circuits (IC) by means of electron beams. In fact, however, several problems have to be eliminated in order to introduce this testing technique into a production line procedure.

In a first step, preconditions have to be met. These are a primary electron (PE) energy where the electron yield is greater than one and a sufficiently low extraction field above the IC. Secondly, as CCVC vanishes within a certain time span caused by charge compensation during electron irradiation, several precautions have to be undertaken. To obtain unfalsified CCVC-micrographs a fast image recording and processing system has to be realized; for IC-internal waveform measurements suitable sampling electronics have to be developed. Besides this, the resulting measurement errors are classified and determined. These are the error due to charge compensation on the passivation layer during electron irradiation, the error due to an incomplete coupling of the line potential to the passivation surface and the error due to capacitive coupling cross talk from neighboring lines.

KEY WORDS: Capacitive coupling voltage contrast, fast image recording and processing system, conventional sampling technique, multisampling technique, sample and hold technique, dynamic charge compensation error, capacitive coupling error, capacitive coupling cross talk.

* Address for correspondence:
E. Kubalek, Universität Duisburg, Fachgebiet Werkstoffe der Elektrotechnik, Kommandantenstr. 60, 4100 Duisburg 1, F.R.G. (Phone No. (0203) 379-3406)

Introduction

The electron beam permits a non-destructive and non-loading test of unpassivated integrated circuits (IC) with high spatial resolution (Crosthwait and Ivy, 1974). There is a great demand to obtain these attractive properties also for passivated IC enabling an incorporation of the electron beam test in a production line procedure.

Then the failure locations can be pinpointed and reasons for certain yield reductions can be determined. So as to develop such a test tool it is necessary to measure IC-internal signals through the passivation layer. Two different procedures are already known.

The first is to apply a high energy electron beam to generate a conductive channel within the passivation layer (Taylor, 1978). By this technique, passivated bipolar devices were tested successfully (Fujioka et al.,1980), whereas the test of MOS-devices resulted in radiation damage (Miyoshi et al.,1982; Görlich and Kubalek, 1985). Such radiation damage can be greatly reduced by blanking the electron beam during digital scanning in the region of sensitive IC-areas (Görlich et al., 1983). But in practice this test technique has not been applied successfully because on one hand it needs very extensive hardware and complex software for automation, on the other hand, the large lateral effective range of radiation damage requires an area consuming IC-design (Reiners et al., 1985).

In contrast to this technique, the capacitive coupling voltage contrast (CCVC) requires a low energy electron beam, thus also enabling one to perform a non-destructive test on passivated MOS-devices (Reiners et al., 1985). The information necessary for testing, *i.e.*, the IC-internal signals, can be determined by capacitive coupling between IC-internal lines and irradiated passivation surface (Crosthwait and Ivy, 1974). In the years following, several authors reported qualitative applications of CCVC

(Kotorman, 1980; Younkin, 1981; Görlich et al., 1982; Ura et al., 1982; Walter et al., 1982; Todokoro et al., 1983) demonstrating the applicability of this technique, although a quantitative theory of CCVC did not exist. In the meantime CCVC is theoretically understood (Görlich et al., 1984). Consequences of this knowledge were hardware modifications which were necessary to make practical use of CCVC as a quantitative electron beam test technique for passivated devices (Görlich et al., 1986; Ookubo et al., 1986). Therefore the electron beam test via CCVC could, in principle, be incorporated in a production line procedure. However, some conditions have to be met. Besides appropriate and improved signal recording and processing equipment, there is a great demand to know the suitable measurement parameters for applying CCVC to electron beam testing. Furthermore, data about the principal measurement errors for this test technique do not exist. The aim of this work is to solve some of the problems outlined above.

First of all, CCVC will be briefly explained and the basic conditions for its appearance introduced. Then follows a detailed description of the necessary hardware modifications and extensions of the electron beam test system to qualify it for testing passivated IC. The principal measurement errors will be illustrated. Two models presented in this work will help to give a quantitative understanding of these measurement errors. From this, the limitations of the applicability of CCVC for testing passivated IC will be derived.

List of symbols

CCCT	capacitive coupling cross talk
CCE	capacitive coupling error
CCVC	capacitive coupling voltage contrast
CST	conventional sampling technique
DCCE	dynamic charge compensation error
FIRPS	fast image recording and processing system
IC	integrated circuit
MST	multisampling technique
PE	primary electron
SE	secondary electron
SHT	sample and hold technique
a	line width
A_B	irradiated area
b	line spacing
C_P	capacitance between buried line and irradiated area A_B
d_P	passivation thickness
d_M	spatial extension of the potential barrier
e	distance of the line to the grounded substrate
E_E	extraction field
E_{PE}	primary electron energy
E_{PEI}, E_{PEII}	primary electron energy where $\sigma = 0$
E_{SE}	energy of the secondary electrons
$F(u_B(t))$	non-linear function of the potential contrast
f_U	upper cut-off frequency
G	achieved gain applying the sample and hold technique
h	height of the line
$h(t)$	normalized primary electron current
$i_{AE}(t)$	absorbed current
i_{BE}	backscattered electron current
$i_{DCST}(\theta_n)$	detected current applying CST
$i_{DMST}(\theta_n)$	detected current applying MST
$i_{DSE}(t)$	detected secondary electron current
i_{PE}	time independent primary electron current
$i_{PE}(t)$	primary electron current
i_{PEO}	primary electron current amplitude
n	index of phase position
N_M	number of averaged waveforms using the MST
N_{PH}	number of samples at a constant phase position
N_{PHC}	N_{PH} for a conventional sampling system
N_{PHM}	N_{PH} for a multisampling system
N_{SE}	energy distribution of the secondary electrons
R	time independent equivalent resistance
$R(t)$	equivalent resistance
t, t', t''	variables of the time
T	period of the line potential
T_A	averaging time
T_M	measuring time
T_{MP}	time span within which the phase position is changed by a microprocessor
T_P	primary electon current pulse width
T_{ST}	storage time
$u_B(t)$	potential barrier
$u_C(t)$	line (conductor) potential
u_{RO}	retarding potential
$u_S(t)$	surface potential
u_{SO}	equilibrium surface potential
δ	secondary electron yield
$\epsilon_0 \cdot \epsilon_r$	permittivity of the passivation
η	backscattered electron yield
θ, θ_n	phase positions
κ	relative dynamic charge compensation error
ν	duty cycle
σ	electron yield
τ_B	measured storage time constant of the bright contrast applying MST
τ_D	measured storage time constant of the dark contrast applying MST
τ_S	simulated storage time contant applying MST

τ_{ST}	storage time constant
$\tau_{ST}(t)$	storage time function
ω_B	lower cut-off frequency of the bright contrast applying MST
ω_D	lower cut-off frequency of the dark contrast applying MST
ω_S	similated lower cut-off frequency applying MST
$\omega_{ST}(t)$	time dependent lower cut-off frequency

Capacitive coupling voltage contrast

The first fundamental precondition for the appearance of CCVC is a suitable primary electron (PE) energy where the electron yield σ , which is the sum of secondary electron (SE) yield δ and backscattered electron (BE) yield η , is greater than one. This results in a positively charged passivation surface and thus in a positive passivation surface potential u_{SO} (state of equilibrium). An electron yield greater than 1 is given for PE energies (E_{PE}) between two energy levels E_{PEI} and E_{PEII}, where σ is equal to 1. For passivation materials normally used, E_{PEII} is smaller than 1.5keV (Seiler, 1983) avoiding radiation damage and enabling a non-destructive test of MOS-devices.

A second fundamental precondition for the appearance of CCVC is a sufficient low extraction field (< 100V/mm) above the IC (Nye and Dinnis, 1985; Görlich et al., 1986). As the measurement errors due to local field effects, such as trajectory contrast and potential barriers (Nakamae et al., 1981) on the contrary are reduced using high extraction fields in the order of 1000V/mm, therefore a compromise is necessary when adjusting the extraction field. Until now no quantitative correlations exist for these contrary tendencies. Only experimental results demonstrate the importance of this second precondition (Görlich et al., 1986).

If both preconditions are satisfied, a.c.-signals in passivated IC are transferred to the passivation surface via capacitve coupling, but they vanish within the storage time T_{ST} due to electron irradiation. A quantitative description of the CCVC is derived by the following formulas (Fig. 1) (Görlich et al., 1986):

- The absorbed current $i_{AE}(t)$ is given by the current balance between the incident PE-current i_{PE}, the detected current of SE, $i_{DSE}(t)$ and the emitted current of the BE, i_{BE}. By means of the backscattered electron yield η the current balance is given as:

$$i_{AE}(t) = (1-\eta)\cdot i_{PE} - i_{DSE}(t) \qquad (1)$$

- The detected SE-current $i_{DSE}(t)$ is determined by PE-current i_{PE}, SE yield $\delta(E_{PE})$ and voltage contrast described by $F(u_B(t))$:

$$i_{DSE}(t) = i_{PE}\cdot\delta(E_{PE})\cdot F(u_B(t)) \qquad (2)$$

where

$$F(u_B(t)) = \frac{\int_{e\,u_B(t)}^{50\ eV} N_{SE}\,dE_{SE}}{\int_{0}^{50\ eV} N_{SE}\,dE_{SE}} \qquad (3)$$

$u_B(t)$ is the potential barrier and is given by the difference between the surface potential $u_S(t)$ and a constant retarding potential u_{RO} (due to an existing microfield or adjusted within a SE-spectrometer):

$$u_B(t) = u_S(t) - u_{RO} \qquad (4)$$

N_{SE} is the energy spectrum of the SE and is calculated in accordance with (Seah, 1969). $\delta(E_{PE})$ considers the dependence of the SE yield on the PE energy (Seiler, 1983).

- Since the passivation layer acts as a dielectric between two electrodes, the irradiated passivation surface area A_B (with surface potential $u_S(t)$) and the line below (line potential $u_C(t)$), this arrangement can approximately be described as an ordinary plate capacitor:

$$\frac{d}{dt}\left[\,u_S(t) - u_C(t)\,\right] = \frac{i_{AE}(t)}{C_P} \qquad (5)$$

where the capacitance:

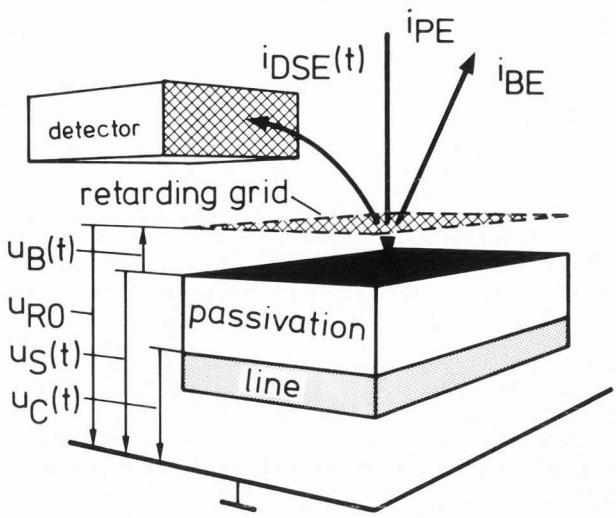

Fig. 1. Cross section of an IC, irradiated by a primary electron beam and definition of the existing potentials and currents

$$C_P = \frac{\epsilon_0 \cdot \epsilon_r \cdot A_B}{dp} \qquad (6)$$

is given by the area A_B, the thickness dp and the permittivity $\epsilon_0 \cdot \epsilon_r$ of the passivation layer.

Based on these eqs.(1)-(6) a computer simulation was performed demonstrating the properties of the CCVC effect and its dependence on relevant parameters (Görlich and Kubalek., 1985; Görlich, et al. 1986).

Modifications in the electron beam test system

Developing an electron beam test system for passivated IC one has to be aware that the information can only be obtained during the storage time T_{ST}. Accordingly, the measuring time T_M, when the signal is detected and processed, has to be much shorter than T_{ST}. This condition is maintained either by extending T_{ST} or shortening T_M.

As the storage time is determined by fixed parameters of the IC under test (passivation material, geometry of the test point and the signal form) (Görlich et al., 1986) and by the PE-current, a longer T_{ST} is only achieved if the PE-current is decreased or the irradiation area A_B is enlarged. However, A_B is fixed for a special test task. For a qualitative CCVC-micrograph of a certain IC-part, the irradiated area is given by the IC-part itself, in a quantitative type waveform measurement however, A_B is a spot which has to be smaller than the IC-internal line. The associated reduction in the PE-current results in a poorer signal-to-noise ratio (SNR) and is therefore limited, also. Only an enlargement of T_{ST} is achieved by the application of the sample and hold technique (Koellen and Brizel, 1983) which yields in the same SNR for lower PE-currents. Therefore the enlargement of T_{ST} is strongly limited.

In contrast, the measurement time T_M can be drastically shortened by use of modified signal processing techniques.

For qualitative CCVC-micrographs, this was already obtained by an incorporation of the fast digital image acquisition system with an information depth per pixel of 1 bit. (Görlich et al., 1986). However this information depth has proven to be insufficient in practice. Consequently an improved fast image recording and processing system (FIRPS) is introduced here and its performance demonstrated.

For a quantitative waveform measurement the time to measure one entire period of the waveform can be reduced by means of the multisampling technique (MST) (Todokoro et al., 1983; Görlich et al., 1986). The principle of this technique and its performance in comparison with the conventional sampling technique (CST) will be discussed quantitatively. It forms the basis for a new theoretical model of CCVC including the used signal processing technique (CST and MST). Under certain conditions this model allows an approximate evaluation of the resulting measurement error using CST or MST, respectively.

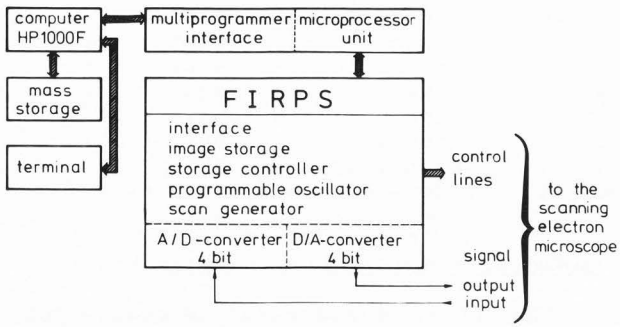

Fig. 2. Blockdiagram of the fast image recording and processing system (FIRPS).

Fast image recording and processing system (FIRPS)

FIRPS permits a CCVC-micrograph to be recorded and stored by way of a digital scan with a maximum pixel frequency of 1.2 MHz. The information depth per pixel is 4 bit (16 levels). The image resolution can be selected from 128 x 128 to 1024 x 1024 pixels. The block diagram of FIRPS is shown in Fig. 2. For image processing a communication between FIRPS and a process computer is enabled via a multiprogrammer interface and a microprocessor unit. With FIRPS, for example, a CCVC-micrograph with 512 x 512 pixels is recorded and stored in $T_M \approx 220$ms, whereas the conventional system takes 60s. In this sense FIRPS first of all enables or at least improves the recording of CCVC-micrographs. Fig. 3 demonstrates the dependence of CCVC on recording (measuring) time T_M at a CMOS frequency divider (passivation SiO_2, thickness dp = 0.8µm) hereby T_M comes to a) 0.22s b) 1.8s and c) 7.1s. The shorter T_M the shorter the time to compensate the influenced charge on the passivation surface by electron beam irradiation and the longer it takes for CCVC to vanish.

FIRPS permits various image processing techniques like comparison, subtraction, filtering of images and is therefore a precondition and a powerful tool for functional and failure analysis of passivated MOS-devices.

Multisampling technique (MST)

High-frequency periodic IC-internal waveforms are measured via CCVC with aid of the MST (Todokoro et al., 1983; Görlich, 1986).

Both CST and MST are sampling tech-

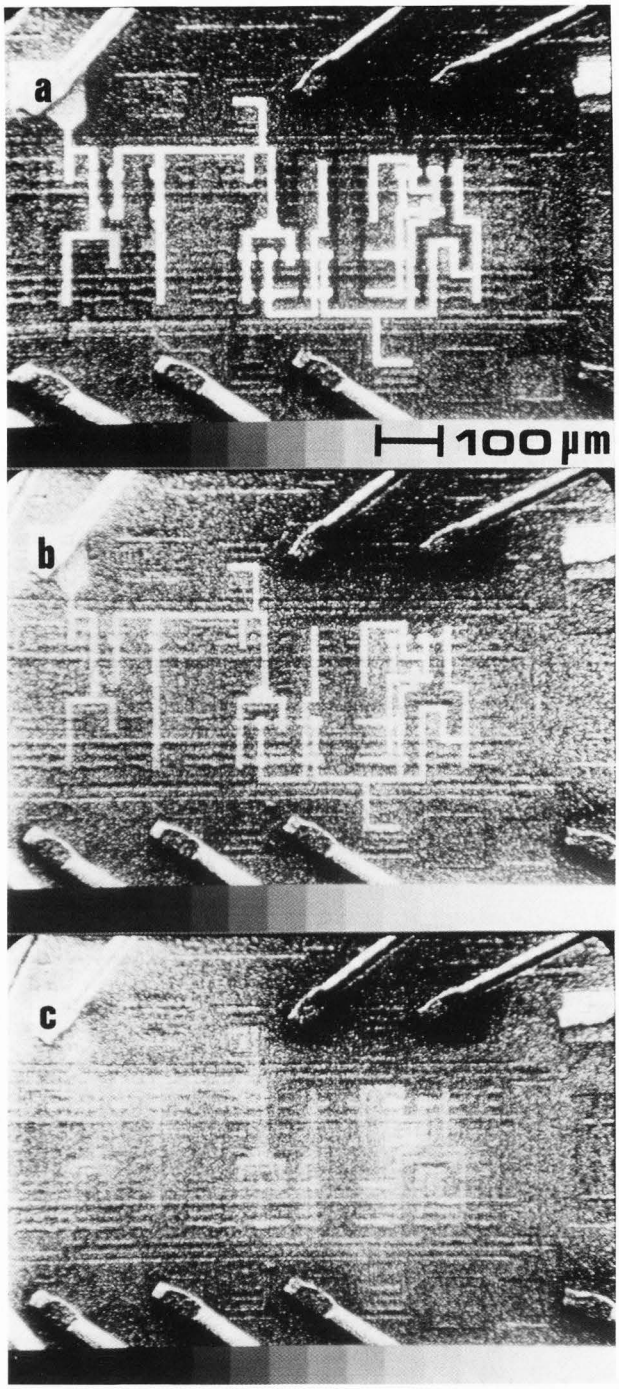

Fig. 3. CCVC-micrographs of a CMOS frequency divider (passivation SiO_2, thickness dp = 0.8µm) using FIRPS after switching on a static voltage. Information depth per pixel is 4 bits (16 levels shown at the picture's bottom). The recording time T_M is varied : 0.22s (a), 1.8s (b) and 7.1s (c).

niques of waveform measurements by means of a synchronous pulsed PE-current. The phase between the waveform and the PE-current pulses is constant and the number of samples in this case is N_{PH}. A measure of the waveform amplitude at this specific phase is the amplitude of the resulting detected SE-current pulses. In order to get the entire waveform, *i.e.*, one period, the phase has to be increased stepwise and at each constant phase the SE-current pulses have to be measured N_{PH} times. The number of phase positions N_S to sample one period T of the waveform has to be high enough to satisfy the sampling theorem (Cooper and McGillem, 1967):

$$N_S \geq 2 \cdot f_U \cdot T \qquad (7)$$

where f_U is the upper cut-off frequency of the IC-internal waveform. Then the measured waveform can completely be reconstructed. Otherwise the waveform is undersampled resulting in a measurement error. If, however, f_U is non existent, *e.g.*, for a rectangular waveform, the high frequency components ($f_U > N_S/2T$) of the measured waveform are distorted and do not reproduce the corresponding frequency components of the rectangular waveform at the line.

However, the way for obtaining a sufficiently high SNR is different for CST and MST. CST makes use of a high number N_{PHC} of samples at a constant phase position and averages the resulting SE-current pulses. With increasing averaging time which is given as $T_A = N_{PHC} \cdot T$, the SNR is more reduced. However, CCVC vanishes faster with increasing T_A , which is equivalent to a longer electron beam irradiation time. From this, a compromise has to be found to get both a sufficiently high SNR and an acceptable measurement error due to dynamic charge compensation on the passivation layer (dynamic charge compensation error DCCE). In practice both requirements cannot be matched applying CST.

In contrast to CST, MST works with a small number N_{PHM} of samples at a constant phase position. The lowest value of N_{PHM} is given by the time T_{MP} where the phase can be changed which is determined by the microprocessor used (Z80, 10MHz clock frequency) and by the software in the multisampling system. Here, the achieved minimum value is $T_{MP} = 49.5\mu s = N_{PHM} \cdot T$. MST in contrast to CST achieves a reduction in noise by averaging N_M completely measured waveforms by aid of a digital storage oscilloscope (Tektronix 7854). By this way each measured waveform and therefore also the averaged waveform are taken with the lowest N_{PHM} resulting in a small DCCE. In contrast, CST uses a high N_{PHC} resulting in a great DCCE although the SNR is identical ($N_M = N_{PHC}$) or even better if $N_M > N_{PHC}$. A restriction for N_M is only given by a reasonable measurement time.

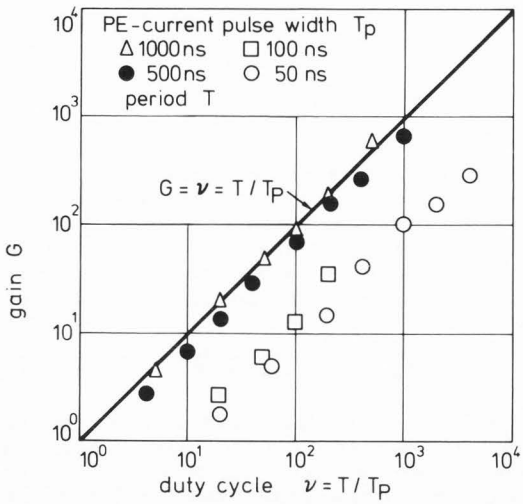

Fig. 4. Correlation between the obtained gain G and duty cycle ν applying a sample and hold circuit.

Sample and hold technique

The sample and hold technique (SHT) which is restricted to electron beam test techniques using a pulsed PE-beam can be employed for both CST and MST. Synchronously with the PE-current pulses, the resulting SE-current pulses are sampled at their maximum and a used sample and hold circuit retain these signal values between two successive samples.

In the CST the SE-current pulses are averaged at each constant phase position. Employing SHT to CST results on the one hand in an amplification of the measured waveform by the gain G (Koellen and Brizel, 1983). If one apply CST or the combination of CST and SHT and if one assumes that the resulting measured signal level is the same in either case, the combination of CST and SHT requires a PE-current which is by a factor of G lower than the one if only CST is applied. In other words, this means, that for the same adjusted PE-current the storage time is increased and thus the DCCE is decreased if the combination of the CST and SHT is used. The achieved gain is given as G = T/Tp which is equivalent to the used duty cycle ν given by the ratio T/Tp. Fig. 4 shows experimental results of these correlations. The expected formula G = ν is only valid for Tp ≥ 1000ns, which is caused by the limited time resolution of the used photomultiplier and head-amplifier, resulting in the same measured SE-current pulse width although Tp is shortened.

In the MST, SHT does not act as an amplifier but is necessary for successful averaging of the measured waveforms. The MST records and averages the entire waveforms N_M times by a digital oscilloscope which is triggered before each waveform is recorded. Without SHT the SE-current is measured directly by the digital oscilloscope via an internal sampling which is not synchronized to the periodic SE-current. This means that due to the high duty cycle the SE-current is mainly sampled at times when no SE-current pulse is existent. Consequently, an averaged waveform cannot be recorded. However, if SHT is applied the oscilloscope always samples the maximum value of the SE-current pulses and averaging of the measured waveforms can successfully be performed.

Measurement errors due to CCVC

The accuracy of the quantitative voltage measurement at passivated IC via CCVC is determined by the measurement errors known from the test of unpassivated IC, the so-called local field effects I and II (Nakamae et al., 1981) but additionally by the measurement errors due to the CCVC. Two different types of these latter errors can be distinguished:

The first DCCE is due to the dynamic behaviour of CCVC and depends on beam parameters, kind of sampling technique (CST or MST) and associated sampling parameters as well as on specimen parameters (passivation material and thickness). This error is discussed in detail by aid of a theoretical model.

The second error is caused by an incomplete capacitive coupling of the line potential to the irradiated passivation surface and by capacitive cross talk from neighboring line potentials. This error is quantified by the charge simulation method (Singer, 1973) for different parameters.

Extended CCVC-model and determination of the dynamic charge compensation error (DCCE)

For a theoretical determination of the DCCE the described CCVC-model (Görlich et al., 1984; Görlich, et al. 1986) has to be extended in respect to the applied sampling technique, replacing the time constant PE-current by a time dependent PE-current and taking into account the specifications of CST and MST. Then the absorbed current changes to:

$$i_{AE}(t) = (1-\eta)\cdot i_{PE}(t) - i_{DSE}(t) \quad (1a)$$

and the detected SE-current can be written as:

$$i_{DSE}(t) = i_{PE}(t)\cdot\delta(E_{PE})\cdot F(u_B(t)) \quad (3a)$$

but the other equations are still valid. As the set of equations (1a),(2),(3a), (4)-(6) includes the non-linear term $F(u_B(t))$ (eqs.(2) and (3a)) and the time variant eq.(3a), the solution would be difficult to find without the aid of a computer. However, the voltage contrast described by the term $F(u_B(t))$ can be approximated by the linear formula:

$$F(u_B(t)) = 1 - \frac{u_B(t)}{50V} \qquad (8)$$

getting now a set of linear equations which can be solved in a closed form. This is provided for the surface potential:

$$u_S(t) = u_{SO} + \exp\left\{ - \int_0^t \frac{dt'}{\tau_{ST}(t')} \right\} \cdot$$

$$\cdot \int_0^t \frac{du_C(t')}{dt'} \exp\left\{ \int_0^{t'} \frac{dt''}{\tau_{ST}(t'')} \right\} dt' \qquad (9)$$

with equilibrium surface potential:

$$u_{SO} = 50V \left\{1 + \frac{\eta - 1}{\delta(E_{PE})}\right\} + u_{RO} \qquad (10)$$

storage time function:

$$\tau_{ST}(t) = \frac{\tau_{ST}}{h(t)} \qquad (11)$$

storage time constant:

$$\tau_{ST} = C_P \cdot R = \frac{\epsilon_0 \cdot \epsilon_r \cdot A_B \cdot 50V}{d_P \cdot |i_{PEO}| \cdot \delta(E_{PE})} \qquad (12)$$

equivalent resistance R and normalized PE-current:

$$h(t) = - \frac{i_{PE}(t)}{|i_{PEO}|} \qquad (13)$$

The correlation between storage time T_{ST} which is defined as span of time where CCVC vanishes and storage time constant τ_{ST} where CCVC is decreased from 100% to 37%, is approximately given as:

$$T_{ST} = 5 \cdot \tau_{ST} \qquad (14)$$

Hence for known device parameters and PE-current eqs.(14) and (12) enable one to determine the storage time T_{ST} easily. Although the calculation of $u_S(t)$ for any line potential and any PE-current pulse form seem to be complicated (eq. (9)), it is possible to draw up a simple electrical equivalent-circuit diagram (Fig. 5). CCVC can now be understood as a high pass filter with storage time function $\tau_{ST}(t)$ and equilibrium surface potential u_{SO} as parameters. The filters lower cut-off frequency (-3dB) is given as:

$$\omega_{ST}(t) = \frac{1}{\tau_{ST}(t)} \qquad (15)$$

and is also a function of time.

In order to get an extended model including the specifications of the used sampling techniques, the SE-current pulses at a constant phase position (signed

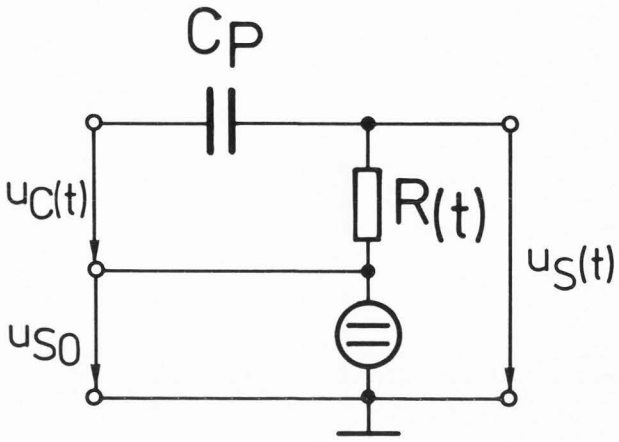

Fig. 5. Electric equivalent-circuit diagram of CCVC for a time dependent primary electron current $i_{PE}(t)$.

by a corresponding time delay θ) have to be determined:

$$i_{DSE}(t,\theta) = \left\{ \frac{\eta - 1}{\delta(E_{PE})} \cdot 50V + u_1(t,\theta) \right\} \cdot \frac{h(t-\theta)}{R} \qquad (16)$$

with

$$u_1(t,\theta) = \exp\left\{ - \frac{1}{\tau_{ST}} \int_0^t h(t'-\theta)dt' \right\} \cdot$$

$$\int_0^t \frac{du_C(t')}{dt'} \exp\left\{ \frac{1}{\tau_{ST}} \int_0^{t'} h(t''-\theta)dt'' \right\} dt' \qquad (17)$$

The measured waveform consists of N_S values assigned by the index n, ($1 \leq n \leq N_S$) and each value is measured during the corresponding constant phase position θ_n. CST makes use of an averaged SE-current $i_{DCST}(\theta_n)$ at a constant phase position θ_n:

$$i_{DCST}(\theta_n) = \frac{1}{T_A} \int_{n \cdot T}^{(n+1) \cdot T_A} i_{DSE}(t,\theta_n)\, dt \qquad (18)$$

Hereby the averaging is started at $n \cdot T_A$ and performed during T_A.

In contrast to CST, MST does not perform an averaging at constant phase position but works with SHT. This means that the SE-current pulses are sampled at their highest values, whereby the last value sampled during the constant phase θ_n is taken at the time $t = \theta_n + n \cdot T_{MP}$ and represents the measured waveform at θ_n:

$$i_{DMST}(\theta_n) = i_{DSE}(\theta_n + n \cdot T_{MP}, \theta_n) \qquad (19)$$

For any line potential, any PE-cur-

rent pulse form and any device and beam parameters the derived model enables a prediction of the resulting measured waveform either for CST or MST.

The storage time constant or the lower cut-off frequency resulting from the application of CST or MST are a measure for the DCCE. Therefore, the applicability of the model using the MST is demonstrated by comparing measured with theoretically calculated dependences of the lower cutoff frequencies for different parameters N_{PH}, N_S and ν. First, the simulated and measured lower cut-off frequencies as a function of the number of samples at a constant phase position N_{PH} are compared. The simulation is performed by aid of a computer, assuming a rectangular, periodic waveform at the line and a rectangular, periodic PE-current. It has to be emphasized that the model cannot make a distinction between a dark contrast time constant τ_D and a bright contrast time constant τ_B which are caused by a positive or a negative voltage swing at the line (Görlich et al., 1986) because the assumed linear approximation of the voltage contrast (eq.(8)) results in only one time constant $\tau_S = \tau_D = \tau_B$. Fig. 6 shows the lower cut-off frequencies which are the reciprocal values of the experimentally obtained time constants τ_D and τ_B and the time constant τ_S obtained by simulation in dependence on the number of samples at constant phase position N_{PHM}. Increasing N_{PHM} causes a linear increase of the cut-off frequencies for both experiment and simulation.

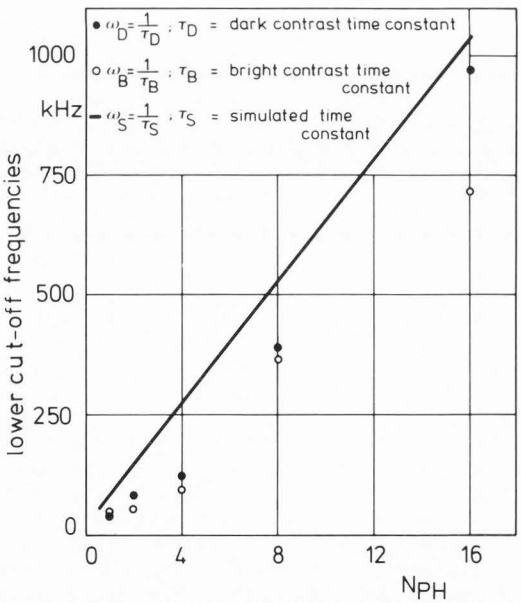

Fig. 6. Lower cut-off frequencies of CCVC applying MST versus number of samples at a constant phase position N_{PH}. E_{PE} = 1.0 keV, A_B = 10μm^2, i_{PEO} = 0.25nA, dp = 1.8 μm, T = 70μs, Tp = 200ns, N_S = 380, δ = 1.02, η = 0.1 and ϵ_r = 4.

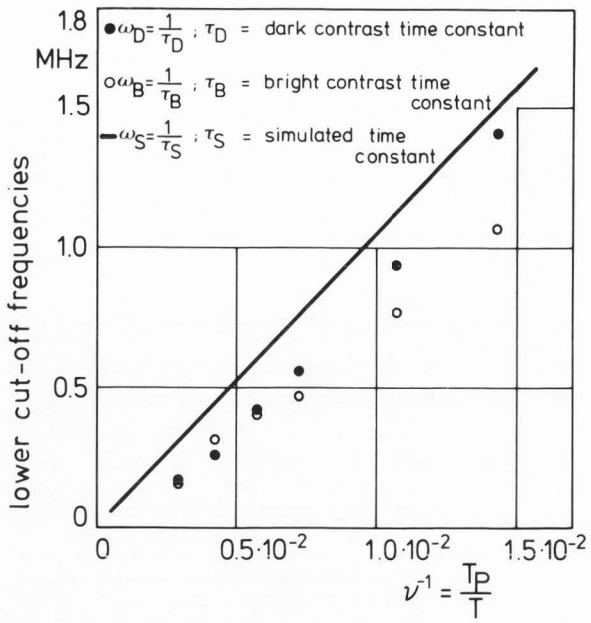

Fig. 7. Lower cut-off frequencies of CCVC applying MST versus reciprocal duty cycle. E_{PE} = 1.0keV, A_B = 10μm^2, i_{PEO} = 0.25nA, dp = 1.8μm, T = 70μs, N_S = 380, N_{PH} = 4, δ = 1.02, η = 0.1 and ϵ_r= 4

However, the corresponding time constants of simulation τ_S are about a factor 1.5 smaller than the measured ones.

Secondly, Fig. 7 shows the dependence of the cut-off frequencies on the reciprocal duty cycle $1/\nu$. With increasing $1/\nu$ the cut-off frequencies become linearly greater but the corresponding simulated time constant τ_S is also about a factor 1.5 smaller than the measured constants τ_D and τ_B.

Therefore a lower DCCE is gained for a small N_{PHM} and a low $1/\nu$. The differences in Fig. 6 and Fig. 7 between experiment and theory are caused on the one hand by the linear approximation for solving the eqs.(1a),(2),(3a),(4)-(6). On the other hand the assumed model of a plate capacitor is no longer valid for waveform measurements, because in this case one electrode of the plate capacitor is represented by the small electron probe, so that electric stray fields will become dominant.

Besides the previously discussed specific parameters of the used sampling technique, the knowledge of the dependence of the storage time on the number of phase positions to sample one period N_S is essential because N_S has to meet two conditions. The first one refers to obtaining a low DCCE and the second one is an N_S high enough to satisfy the sampling theorem. Since the hardware of the developed MST is not designed to vary N_S, the correlation between cut-off frequency, as a measure for the storage time and thus for DCCE and N_S is only simulated. With

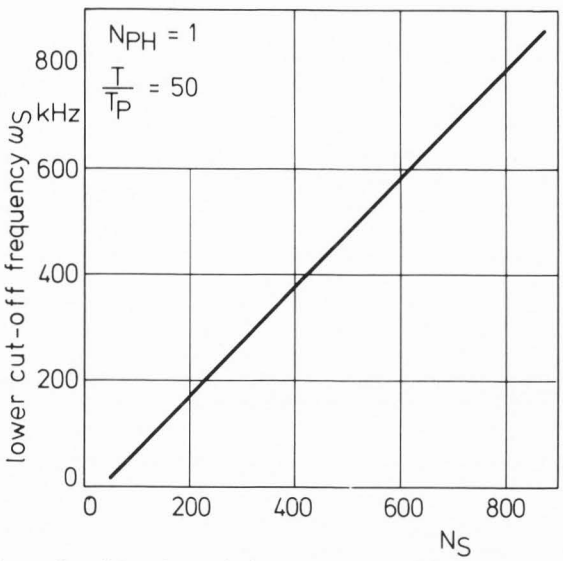

Fig. 8. Simulated lower cut-off frequency of CCVC applying MST versus number of phase positions to sample one period N_S. E_{PE} = 1.0keV, A_B = 10μm^2, i_{PEO} = 0.25nA, d_P = 1.8μm, T = 70μs, T_P= 1.4μs, N_{PH} = 1, δ = 1.02, η = 0.1 and ϵ_r = 4.

increasing N_S the lower cut-off frequency becomes also linearly greater (Fig. 8). This means DCCE is lower for small N_S, but in respect to the sampling theorem a higher N_S is desirable. Consequently, a compromise for the number N_S has to be found.

In order to get a handy formula that enables a prediction of the resulting storage time constant τ_S and thus for DCCE by using CST and MST, a special waveform at the line and a special PE-current are assumed. A simplified determination of τ_S and DCCE is possible for a constant line potential and a rectangular periodic PE-current with pulse width T_P and period T. By aid of the model the following storage time constant τ_S can for both techniques be calculated to:

$$\tau_S = \tau_{ST} \cdot \frac{T}{T_P} \cdot \frac{1}{N_{PH} \cdot N_S} \qquad (20)$$

where the number of samplings at a constant phase position N_{PH} is different for each sampling technique. For CST, $N_{PH} = N_{PHC}$ is given as the ratio of averaging time T_A and period T:

$$N_{PHC} = \frac{T_A}{T} \qquad (21)$$

whereas for MST, $N_{PH} = N_{PHM}$ is given as the ratio of the span of time T_{MP} to change a phase position and period T:

$$N_{PHM} = \frac{T_{MP}}{T} \qquad (22)$$

As $T_{MP} \ll T_A$ is valid the resulting storage time constant τ_S for MST is much greater than for CST. Eq.(20) is in a rather good agreement with the results which were calculated directly by the computer (Figs. 6 - 8).

A greater τ_S is correlated with a lower DCCE. This correlation is determined for a relative DCCE assigned by κ, that is, the normalized decay of the measured waveform within the period T. The calculation is performed under the same conditions as for τ_S by aid of the model:

$$\kappa = 1 - \exp\left[\frac{T}{\tau_S}\right] \qquad (23)$$

Thus for the assumed special constant line voltage and rectangular periodic PE-current, κ can be interpreted as an exponential decay with a time constant τ_S during a time span T. In order to get a nearly unfalsified waveform measurement, κ has to be much lower than 1. Then eq. (23) can be approximated by:

$$\kappa \approx \frac{T_P}{\tau_{ST}} \cdot N_{PH} \cdot N_S \qquad (24)$$

Applying eqs.(24) and (12) allows a proper choice of beam parameters ($|i_{PEO}|$, $\delta(E_{PE})$, A_B) and measurement parameters (T_P, N_{PH}, N_S) resulting in a DCCE lower than κ.

Measurement error due to incomplete capacitive coupling and capacitive coupling cross talk

The model previously discussed is based on the assumption of an ideal plate capacitor, coupling the full voltage swing at the buried line to the passivation surface. However, at small line geometries the coupled voltage swing was found to be less than the voltage swing at the buried line, and shows a dependence on the potentials at the neighboring lines (Todokoro et.al, 1983; Ookubo et. al, 1986). These effects are called capacitive coupling error (CCE) and capacitive coupling cross talk (CCCT), respectively. The reason for CCE and CCCT is the increased stray field of dielectric displacement with decreasing line geometries. This causes a distribution of the influenced charges also besides the projection of the line onto the passivation surface.

CCE and CCCT have been treated quantitatively applying the charge simulation method (Singer, 1973) to the 2-dimensional model shown in Figs. 9 a,b.

This model consists of three parallel lines of the width a, the spacing b, the height h and the distance e to the grounded substrate, covered with a SiO_2 passivation layer of the thickness dp.

Since the voltage swing at the passivation surface only depends on the line potentials and line environment, the sur-

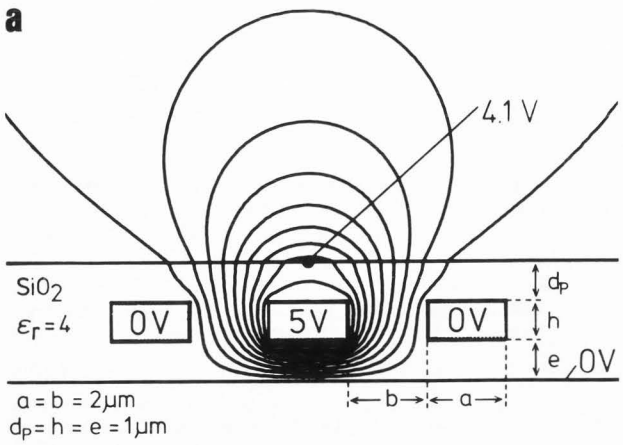

capacitive coupling error : 0.9V

capacitive coupling cross talk : 0.69V

Fig. 9. 2-dimensional model of a passivated IC with lines in one level, and equipotential lines (distance 0.5V) showing: a) the capacitive coupling error CCE: (5V - 4.1V = 0.9V) b) the capacitive coupling cross talk CCCT: (4.79V - 4.1V = 0.69V).

face potential is calculated without the influence of the electron irradiation (causing DCCE) and the extraction field.

Fig. 9a shows the calculated equipotential lines (distance 0.5V) for an arrangement of three lines with 2µm width and spacing and passivation with 1µm SiO_2. The equipotential lines show that the coupled voltage swing from 0V to 5V at the passivation surface is by 0.9V smaller than the voltage swing at the buried centre line. From this the CCE is defined as the difference of the voltage swing at the centre line and the coupled voltage swing at the passivation surface on the condition, that the neighboring lines are at ground potential.

A correction of the CCE by calibration for a fixed geometry is only successful if the neighboring lines remain at constant potential.

Fig. 9b shows an increase of the surface potential by 0.69V if the neighboring lines are also switched from 0V to 5V. From this the CCCT is defined as the increase of the surface potential if the neighboring lines are switched from 0V to the potential of the centre line.

As CCE and CCCT are strongly influenced by the device geometry Fig. 10 shows CCE and CCCT normalized to the voltage swing at the buried lines (same for centre and neighboring lines) as a function of the line width equal to line spacing and for different passivation thicknesses. For a constant passivation thickness and line width and spacing about 4µm, CCE and CCCT are below 20%, but start to increase with smaller line geometries. Future line geometries (a=b= 0.5µm) will show a CCE and a CCCT in the order of 50% depending on passivation thickness. A thicker passivation layer causes an increase of CCE and CCCT.

Application of the CCVC to the analysis of multi-level interconnection devices will be even more critical because CCE and CCCT start to increase at significantly larger line geometries. At 0.5µm line width and typical spacing values are in the order of 90% (Herrmann and Kubalek, 1986). On the assumption that the CCE is calibrated which provides fixed environment of the test point, the ratio

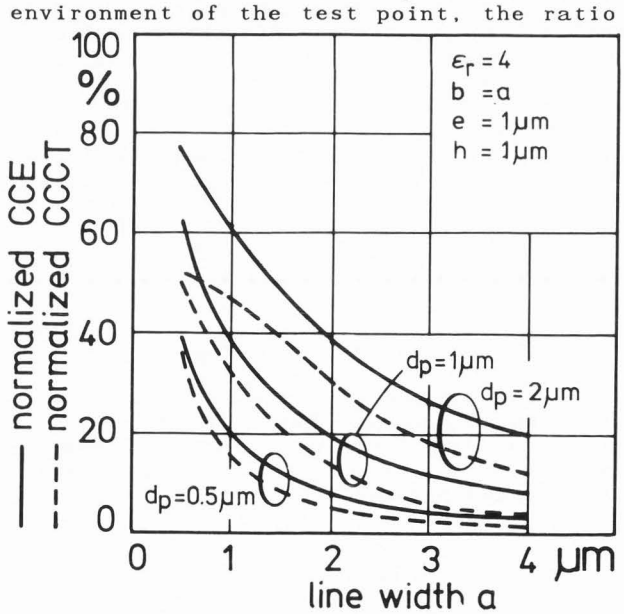

Fig. 10. Capacitive coupling error (CCE) normalized to the potential of the centre line and capacitive coupling crosstalk (CCCT) normalized to the potential of the neighboring lines as a function of line width for different passivation thicknesses according to the model in Fig. 9.

of cross talk and the coupled voltage is the relative measurement error caused by the cross talk. If the maximum error shall be 50% for a logic state analysis and 5% for a quantitative waveform measurement, the following statements can be made if the line width is equal to line spacing (Herrmann and Kubalek, 1986):

i) For all lines in the upper interconnection level:
   - Testing via quantitative waveform analysis is possible if the line width is at least four times the passivation thickness.
   - Testing via logic state analysis is possible if the line width is greater than the passivation thickness.

ii) For the neighboring lines in the upper level and the measurement line on level below:
   - Testing via quantitative waveform measurement is not possible for line geometries used in VLSI devices
   - Logic state analysis is restricted to line widths equal to line spacings greater than 3µm to 5µm depending on passivation thickness.

With a view to future trends in IC-technology these investigations show the limitations of CCVC application to failure analysis of passivated IC.

Although a correction of CCE and CCCT by a calibration seems to be possible, the necessity to find the measurement point with the same environment as the reference structure and the necessity to measure the signals of the neighboring lines do still exist. As especially for multi-level interconnection devices the test access of the electron probe is not given anymore, a design for electron-beam testability has to insure, that all critical paths within the IC will be led to the uppermost interconnection level.

Conclusions

Electron beam testing via CCVC is, in principle, applicable to a non-destructive testing of passivated integrated circuits. A suitable primary electron energy and a sufficiently low extraction field are preconditions for the appearance of CCVC. As the charge influenced on the passivation surface by an a.c.-line potential is compensated during electron irradiation, CCVC vanishes within a storage time or at least the performed measurement is falsified. This dynamic charge compensation error (DCCE) can drastically be reduced by use of appropriate signal processing hardware. In order to obtain unfalsified CCVC-micrographs a fast image recording and processing system is realized and for IC-internal waveform measurements the conventional sampling technique (CST) is replaced by the multisampling technique (MST). A theoretical model describing CCVC as well as the specifications of the used sampling technique (CST or MST) allows a quantitative evaluation of DCCE. From this DCCE increases linearly with primary current pulse width, number of samples at a constant phase position, number of phase positions to sample one period of the waveform at the line and decreases linearly with increasing storage time. Experiments comply with these results. In the case of small line geometries the coupled voltage swing on the passivation surface is lower than the one at the buried line and depends also on the potentials at the neighboring lines. Both effects resulting in a capacitive coupling error (CCE) and in a capacitive coupling cross talk (CCCT) are due to the electric stray fields and become even dominant at these small line geometries. CCE and CCCT are also treated quantitatively by a theoretical model. This model predicts that quantitative waveform measurements are possible if the line width is at least four times the passivation thickness but logic state analysis can be performed if the line width is greater than the passivation thickness. However, for lines in a lower level and neighboring lines in the upper level a quantitative waveform measurement is impossible at lines in IC while the logic state analysis is still reasonable for line widths equal to line spacings greater than 3µm to 5µm depending on passivation thickness.

Acknowledgements

The authors would like to thank L. Herzog and M. Bourquardez for the development of the fast image recording and processing system and the multi-sampling system, respectively.

References

Cooper GR, McGillem CD. (1967). Methods of Signal and System Analysis. Holt, Rinehart and Winston Inc., New York, 131 - 150.

Crosthwait DL, Ivy FW. (1974). Voltage contrast methods for semiconductor device failure analysis. Scanning Electron Microsc. 1974: 935 - 940.

Ekuni M, Komoto Y, Gobara T, Harada Y. (1986). Dynamic testing of a passivated device with electron beam tester. Proc. XIth Cong. on Electron Microscopy, Kyoto; 629 - 630.

Fujioka H, Nakamae K, Ura K. (1980). Function testing of bipolar IC's and LSI's with the stroboscopic scanning electron microscope. IEEE Solid State Circuits, SC-15, 177 - 183.

Görlich S, Menzel E, Kubalek E. (1982). Capacitive coupling voltage contrast . In: Beiträge zur elektronenmi-

kroskopischen Direktabbildung von Oberflächen, BEDO, 15, 133 - 142.

Görlich S, Postulka E, Kubalek E. (1983). Window scan mode for testing passivated MOS-devices. In: Microcircuit Engineering, Proc. Int. Conf. Microlithography, Cambridge, Ahmed H, Cleaver JRA, Jones GAC (eds), Academic Press, London, 493 - 500.

Görlich S, Herrmann KD, Kubalek E. (1984). Basic investigations of capacitive coupling voltage contrast. In: Microcircuit Engineering, Proc. Int. Conf. Microlithography, Berlin, Academic Press, London, 451 - 460.

Görlich S, Kubalek E. (1985). Electron beam induced damage on passivated metal oxide semiconductor devices. Scanning Electron Microsc. 1985; I: 87 - 95.

Görlich S. Herrmann KD, Reiners W., Kubalek E. (1986). Capacitive coupling voltage contrast. Scanning Electron Microsc. 1986; II: 447 - 464.

Herrmann KD, Kubalek E. (1986). Some aspects concerning design for e-beam testability. In: Microcircuit Engineering 1986, Proc. Int. Conf. Microlithography, Interlaken, 512 - 522. Lehmann HW, Bleiker CH. (eds) North Holland, Amsterdam

Koellen DS, Brizel KW. (1983). Improved signal to noise ratio with sample and hold in the voltage contrast mode using a scanning electron microscope. Scanning Electron Microsc. 1983; IV: 1605 - 1609.

Kotorman L. (1980). Non-charging electron beam pulse prober on FET wafers. Scanning Electron Microsc. 1980; IV: 77 - 84.

Miyoshi M, Ishikawa M, Okumura K. (1982). Effects of electron beam testing on the short channel metal oxide semiconductor characteristics. Scanning Electron Microsc. 1982; IV: 1507 - 1514.

Nakamae K, Fujioka H, Ura K. (1981). Local field effects on voltage contrast in the scanning electron microscope. J. Phys. D. Appl. Phys., 14, 1939 - 1960.

Nye P, Dinnis A. (1985). Extraction field and oxide charging in voltage contrast systems. Scanning; 7,3, 117 - 124.

Ookubo K, Goto Y, Fukurawa Y, Inagaki T. (1986). Quantitative voltage waveform measurement technique for an IC-internal electrode with a passivation film. Proc. XIth Cong. on Electron Microscopy, Kyoto; 631 - 632.

Reiners W, Görlich S, Kubalek E. (1985). On the Primary Electron Energy Dependence of Radiation Damage in Passivated NMOS Transistors. Inst. Phys. Conf. Ser.; 76, 507 - 512.

Seah MP (1969). Slow electron scattering from metals. Surface Science 17, 132 - 160.

Seiler H. (1983). Secondary electron emission. In: Electron Beam Interaction With Solids, DF. Kyser, H. Niedrig , DE. Newbury, R. Shimizu (eds). SEM Inc., Chicago IL, 60666. 33 - 42.

Singer H. (1973). Berechnung von Hochspannungsfeldern mit Hilfe von Flächenladungen (Calculation of high-tension fields by use of surface charges). Habilitationsschrift Techn. Univ. München.

Taylor DM. (1978). The effect of passivation on the observation of voltage contrast in the scanning electron microscope . J. Phys. D: Appl. Phys., 11, 2443 - 2454.

Todokoro H, Fukuhara S, Komoda T. (1983). Stroboscopic scanning electron microscope with 1 keV electrons. Scanning Electron Microsc. 1983; II: 561 - 568.

Ura K, Fujioka H, Nakamae K, Ishisaka M. (1982). Stroboscopic observation of passivated microprocessor chips by scanning electron microscopy. Scanning Electron Microsc. 1982; III: 1061 - 1068.

Walter MJ, Eldering CA, Krevis KM, Haberer IR. (1982). Internal node testing by tester aided voltage contrast. In: Proceedings of ISTFA 1982, International Symposium for Testing and Failure Analysis, Torrance, CA, 156 -161.

Younkin D. (1981). Phase dependent voltage contrast - An inexpensive SEM addition for LSI failure analysis. 19th Ann. Proc. Reliability Physics, IEEE. 264 - 268.

Discussion with Reviewers

L. Kotorman: With the FIRPS you report max. pixel frequency of 1.2 MHz, what major difficulties would you envision if this rate was to be increased even higher?

Fast recording and processing helps, but would not be limited by SNR considerations which calls for efficient fast detectors?

Authors: If the maximum pixel frequency is increased by improving all units of FIRPS (Fig. 2) the major difficulty is caused by the scan coils of the scanning electron microscope because they are only designed for TV-scan-frequencies. As the image recording is performed in real time the bandwidths of the photomultiplier and amplifiers used have also to be wide enough. A wide bandwidth, however, results in a worse SNR so that more images have to be recorded and averaged to get a sufficiently high SNR. Especially the averaging of images is a time consuming process. Thus an increased detection bandwidth leads to a longer time to record a CCVC-micrograph.

The recording time can be reduced by use of efficient detectors and low noise amplifiers. Therefore, fast efficient detectors have to be applied to get both a long storage time of CCVC and an economic recording time.

L. Kotorman: What primary beam energy and current was used to obtain the CCVC micrographs on Fig. 3? Was only the recording time duration changed between these results?
Authors: The primary electron energy was 1.2 keV and the primary electron beam current was 1.1 nA. All parameters were constant except that the recording time was increased to demonstrate its influence on CCVC.

L. Kotorman: In your experimental setup what is the detector arrangement and what practical detection efficiency could you approximate, please?
Authors: We used an Everhart-Thornley detector and Feuerbaum type spectrometer (Fig. 11) with a spectrometer constant of approximately $2 \cdot 10^{-7} V\sqrt{As}$.

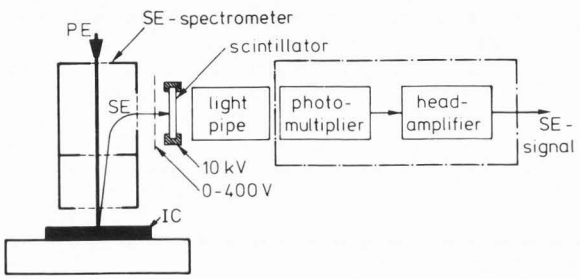

Fig. 11. Detector arrangement

L. Kotorman: The nonlinear nature of the Voltage Contrast F ($u_B(t)$) is resulting from the energy distribution of the secondary electrons as you made some reference to this in the text. However, one examining these distributions finds that the vast majority of the secondary electrons exist from the sample with less than 10 eV energy. If I understand it correctly, in order to simplify the calculations you are replacing this energy distribution with a rectangular one extending from 0 to 50 eV and arriving to the formula of

$$F(u_B(t)) = 1 - \frac{u_B(t)}{50\ V}$$

If this simplification is necessary why not use a rectangular distribution extending from something like 0 to 10 eV; or would perhaps a triangular shape distribution give a much better approximation yet?
Authors: As only an analytical solution of the equations which describe the extended CCVC-model enables the direct derivation of a formula for the calculation of the DCCE (eq.(23) and eq.(24)), this simplification is necessary.

Following the definition of the SE-energy distribution we decided to take the rectangular distribution extending from 0 to 50eV. Your suggestion to take a rectangular one extending from 0 to 10eV is indeed a better approximation for most materials, but increases the lower cut-off frequencies by a factor of 5. This results in a greater discrepancy between theory and experiment and could be explained by the simplifications which are made in the model.

A triangular SE-energy distribution is certainly a better approximation but it would result in a non-linear function $F(u_B(t))$ excluding a simple analytical solution.

H. Todokoro: Miyoshi, et al. reported the Random Sampling Technique that improves the error due to the CCVC at Osaka Testing Symposium, '85. How does your model explain this effect?
Authors: According to eq.(24) the DCCE is reduced by decreasing the numbers N_{PH} and N_S. If the Random Sampling Technique is applied (Ookubo et al., 1986) the number of samples at a constant phase position N_{PH} is not reduced as with MST but N_{PH} has nearly the same value as for the CST (1024). However, due to the random sampling of the waveform at the line, this waveform is transformed into one consisting of higher frequency components. As most of these components are now higher than the lower cut-off frequency ω_{ST} the measured waveform is less falsified. The eqs.(20) - (24) are also valid applying the Random Sampling Technique because both the random and conventional sampling of a constant line voltage which is assumed here result in the same falsification of the detected SE-current. In this case the Random Sampling Technique does not have any advantage. It is worse than the MST because N_{PH} is normally much higher. Therefore, it seems to be the best to combine the MST with the Random Sampling Technique to make use of the advantages of both techniques.

A quantitative description of the Random Sampling Technique can be achieved if the random behaviour of the phase positions is considered in the proposed model.

H. Todokoro: We have used the window probing for CCVC measurements to increase the effective irradiated area A_B. Is there any difference between the window probing and the probing real metal plate on the passivation layer with the same irradiated area A_B?
J. Beall: What effect would a conductive film, *i.e.* beam deposited carbon square area overlaying the measured conductor, have on detected secondary electron current? Would it improve the mobility of surface charge to a fixed point beam landing on the carbon square?
Authors: We did no experiments in this field, but an improvement of the waveform measurement by use of a metal plate was

recently reported (Ekuni et al, 1986). We think if one works in the scan-mode the resulting storage time is the same for the window probing and the probing real metal plate or the beam deposited carbon square area, respectively. However, probing the specimen in the spot mode might show a difference. Using a real metal plate the influenced charge on the whole plate can be compensated because the carriers in the plate are mobile. Otherwise, only the charge within the irradiated spot can be compensated. Thus in the spot mode the metal plate leads to an increased effective irradiated area.

A.R. Dinnis: In some cases, dynamic voltage contrast through passivation remains visible indefinitely even with a 1kV beam accelerating voltage, provided the extraction voltage is adjusted suitably. Have you observed this and can you give some explanation?

Authors: Yes, we observed this behaviour of CCVC by investigating the dependence of the storage time on primary electron energy (Görlich et al., 1986).

For passivation materials normally in use the primary electron energy of 1keV means that the secondary electron yield δ is slightly greater than 1. Thus there is approximately a balance between primary electron current and secondary electron current (equilibrium). The surface potential is then given as $u_{SO} \approx 0$. Higher values of δ would result in $u_{SO} > 0$ (see eq.10). Especially in the case of $u_{SO} \approx 0$, negative voltage swings at the buried line cannot change the SE-current because if $u_{SO} \approx 0$ it has just taken its maximum. Therefore, the absorbed current $i_{AE}(t)$ does not change either and the influenced charge on the surface cannot be compensated. This results in an indefinite storage time of CCVC. As both, the primary electron energy and the extraction field, determine the surface potential in the equilibrium state the extraction voltage has to be suitably adjusted.

A.R. Dinnis: The charging of the passivation surface with a low-voltage beam and an extraction field is a very complex process requiring further investigation. It is certainly undesirable to have an electrode at about 1kV at 1mm from the specimen surface while if the electrode is at 100V or less the charging problem is, as you say, much less. Do you have any comments on how much the problem is related to the extraction field strength and how much to the absolute value of the extraction voltage? For example, if the 100V extractor electrode were moved to 100 microns from the surface, would the effect be as bad as with the 1kV electrode at 1mm ?

J. Beall: You mentioned using a low extraction field above the IC. Would you describe the configuration of the energy spectrometer used and how the proper extraction voltage is determined?

D. Koellen: According to the paper, a fundamental precondition for CCVC is a weak extraction field. What are the reasons for this? Could one use a magnetic rather than an electrostatic field?

Authors: Besides an appropriate primary electron energy ($\delta > 1$) the applied extraction field determines the surface potential. As $\delta > 1$ and if the back-scattered electrons are neglected the equilibrium is reached if the number of SE is equal to the number of PE. However, this is only possible when the potential barrier u_B is positive which forces some SE back to the passivation surface. A positive u_B means a positive equilibrium surface potential u_{SO}. This effect is quantitatively given by eq.(10) demonstrating the dependence of u_{SO} on $\delta(E_{PE})$ if no extraction field is applied. If an extraction field exists the potential barrier is superimposed by this field. At the first moment when the extraction field is applied the potential barrier is decreased because u_{RO} is more positive (Fig. 1) resulting in a more positive surface potential. The equilibrium is reached if u_B is the same as before without extraction field. This behaviour of u_S in the equilibrium state can be described by eq. (10):

$$u_{SO} = 50V \cdot \left[1 + \frac{\eta - 1}{\delta(E_{PE})}\right] + E_E \cdot d_M \quad (25)$$

where u_{RO} is given by the extraction field E_E and the spatial extension of the potential barrier above the passivation surface d_M. The values of d_M are correlated with the dimensions of the test-point and its vicinity. For example if $E_E = 100V/mm$ and assuming $d_M = 100\mu m$ the surface potential changes by about 10V. The higher the extraction field and the larger the test points the more positive is the surface potential. For quantitative waveform measurements this means that the output voltage of the used linearization unit has to be adjusted to high positive values to achieve a reasonable working point on the $i_{DSE}(u_B)$-curve of the spectrometer.

More information about this topic requires further investigation. Especially, it is desirable to know the influence of the geometry of the test points, beam size, extraction field strength and extraction voltage on the surface potential and the consequences arising for the electron beam test of passivated devices.

D. Koellen: Please describe your SEM equipment and typical operating parameters (beam current, extraction field strength, beam-on time, acceleration voltage, etc.). What type of electron

spectrometer do you use?
Authors: We used a Cambridge S180 scanning electron microscope equipped with a beam blanking system, a Feuerbaum type spectrometer and a standard Everhart-Thornley detector. Typical operating parameters for CCVC applications are an extraction field range of 50V/mm to 100 V/mm, an acceleration voltage range of 0.7kV to 2kV, a primary electron beam current of approximately 1nA and a minimum primary electron current pulse width of 10ns.

D. Koellen: CCE and CCCT are treated in a theoretical model shown in Fig. 9. In this figure the passivation is shown to be planar. In real devices, the passivation is very conformal to the underlying metal lines with a slightly greater thickness at the top of the metal. Does this modify the model used for CCE and CCCT since the conformal shape is likely to skew the equipotential lines? Would this also affect the extended model for CCVC, especially where the electron beam size is nearly the same as the metal linewidth?
J. Beall: Were effects of glassivation surface topography and beam deposited hydrocarbon also significant contributors to DCCE?
Authors: We agree that the topography of the passivation will cause slightly different values for CCE and CCCT, since the voltage drop in the passivation layer is smaller than the one in the vacuum. There are still a lot of factors, *e.g.* other line geometries (line crossings) or different thicknesses of the oxide layers which also influence these errors.

In the same way DCCE is slightly changed if topography is existent. The calculation of the effective capacitance (eq.(6)) of the passivation layer is more difficult because now the topography has to be considered.